

Superradiance of High Density Frenkel Excitons at Room Temperature

H. Z. Wang, X. G. Zheng, F. L. Zhao, Z. L. Gao, and Z. X. Yu

Institute for Laser and Spectroscopy, Zhongshan University, Guangzhou 510275, China

(Received 21 June 1994)

Superradiance of high density Frenkel excitons in an *R*-phycoerythrin single crystal is observed at room temperature for the first time. No fluorescence is observed except the emission at the sharp exciton band when the superradiance of excitons occurs, and the higher the pump density, the sharper the emission bandwidth. A redshift and a blueshift are observed at the rise time and the fall time of the emission pulse, respectively. The experimental results also imply deformed-boson properties of high density Frenkel excitons.

PACS numbers: 87.22.Fy, 42.50.Fx, 71.35.+z, 78.47.+p

Superradiance is a phenomenon of collective spontaneous emission of light arising from an ensemble of optically excited systems. It was predicted in 1954 [1], and its first experimental evidence was reported in 1973 [2]. Since then, much work has been done to investigate and interpret the properties of superradiance both experimentally and theoretically. Superradiance from gaseous systems of atoms and molecules was studied first [3,4], followed by that from doped molecular crystals [5,6] and O_2^- -centered crystals [7–9]. In recent years, superradiance of excitons has been an attractive subject. Much interest has been stimulated by theoretical studies on systems with reduced dimensionality [10–14]. Some preliminary studies are focused on the superradiance of Wannier excitons in semiconductor microcrystallites theoretically [15] and experimentally [16]. On the other hand, superradiance of Frenkel excitons has only been observed in *J* aggregates of dye at low temperature [17,18]. However, a *J* aggregate is stable only under low excitation. High or complete population inversion will make this system unstable [12]. In this work, superradiance of high density Frenkel excitons in an *R*-phycoerythrin (*R*-PE) single crystal is observed at room temperature for the first time. The spectral and temporal properties of Frenkel exciton superradiance at high pump density are studied.

Moreover, it is well known that both Frenkel and Wannier excitons behave as pure bosons at low density. At high density and low temperature, Wannier excitons in the indirect-gap semiconductors silicon and germanium condense into a fermionic electron-hole liquid. In recent years, Bose-Einstein condensation of biexcitons in direct-gap CuCl and free excitons in Cu_2O has been studied theoretically and experimentally [19–21]. However, the quantum statistics of high density Frenkel excitons lacks experimental studies, and the theoretical studies have not reached a consensus [14,22–24]. The experimental results in this work will be conducive to understanding the quantum statistics of high density Frenkel excitons.

R-PE is an important phycobiliprotein of photosynthetic antennae in red algae. The experimental results in this work also imply that excitons play an important role in

excitation energy transfer in the photosynthetic antennae of algae.

Our time-resolved fluorescence experiments have been performed with a frequency-doubled cw mode-locked Nd:YAG laser as an excitation source, and a synchroscan streak camera (Hamamatsu Model C1587, 10 ps resolution) connected to a polychromator as a recorder; thus the spectral and temporal characteristics can be recorded simultaneously. Superradiance experiments have been conducted with a frequency-doubled single pulse mode-locked Nd:YAG laser as a pump source and a single sweep streak camera (Hamamatsu Model C1587, 2 ps time resolution) connected to a polychromator as a recorder. The pulse duration of the single pulse mode-locked Nd:YAG laser is 30 ps. Superradiance experiments have been carried out at room temperature.

At low excitation density and room temperature, the fluorescence of an *R*-PE single crystal or microcrystal is a broadband emission with a bandwidth of 50 nm and a peak at 580 nm, as shown in Fig. 1(a). It is almost the same as that of *R*-PE in phosphate buffer solution ($pH \sim 7$). Figure 1(b) shows the fluorescence of the *R*-PE microcrystal at 77 K, in which a sharp exciton band appears at 600 nm with a bandwidth of 9 nm (for the bulk crystal, the bandwidth is 15 nm). The fluorescence decay (at 600 nm) of the *R*-PE microcrystal at 77 K consists of two components: one is the short lifetime component of broadband fluorescence peaking at 580 nm, and the other is the long lifetime component of the sharp exciton band with a lifetime of 1.9 ns. The excitonic fluorescence excitation spectrum, as shown in Fig. 2, is detected at 77 K. In order to eliminate the disturbance of light scattering and the short lifetime broadband fluorescence, the fluorescence is dispersed by the streak camera and detected at 600 nm during 1.8–2.0 ns.

When the pump density increases, a sharp exciton band at 600 nm appears at room temperature, as shown in Fig. 3(a). When the pump density is up to 7 GW/cm^2 , exciton superradiance occurs at room temperature. The phenomena are described as follows.

(1) The emission only appears in the sharp exciton band, and no emission occurs at the wavelength of the

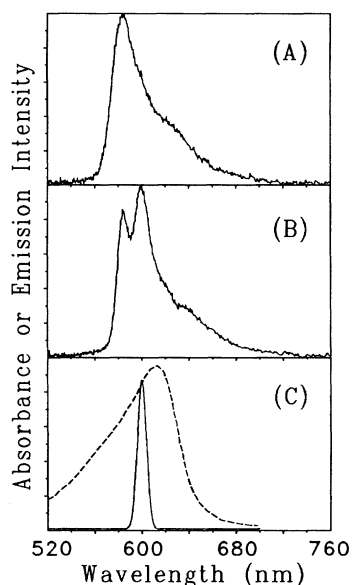


FIG. 1. Fluorescence spectra of an *R*-PE microcrystal at low excitation density (0.1 W/cm^2) and the absorption spectrum of *C*-phycoerythrin (*C*-PC). (a) Fluorescence of *R*-PE microcrystal at room temperature. (b) Fluorescence of *R*-PE microcrystal at 77 K. (c) Exciton band of *R*-PE microcrystal decomposed from (b) (solid line), and absorption spectrum of *C*-PC (dashed line).

broadband fluorescence peaking at 580 nm, as shown in Fig. 3(b).

(2) The peak intensity of the emission (I_{peak}) is almost proportional to the square of the pump intensity (I_{pump}), i.e., $I_{\text{peak}} \propto I_{\text{pump}}^{2-\beta}$, where $\beta < 0.5$ and its exact value is dependent on I_{pump} . First, this excludes cases of exciton-exciton annihilation and amplified spontaneous emission. Second, the thickness of the excited region depends on the pump density; therefore the total number of chromophores or the total exciton number (N) in the excited region is proportional to the pump density, i.e., $I_{\text{peak}} \propto N^{2-\beta}$, approaching ideal Dicke superradiance where $I_{\text{peak}} \propto N^2$.

(3) At room temperature and low pump density, the fluorescence lifetime of *R*-PE at 580 nm is 319 ps, as

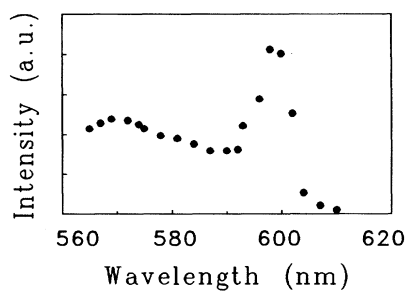


FIG. 2. Excitonic fluorescence excitation spectrum of *R*-PE microcrystal detected at 600 nm during 1.8–2.0 ns after excitation at 77 K.

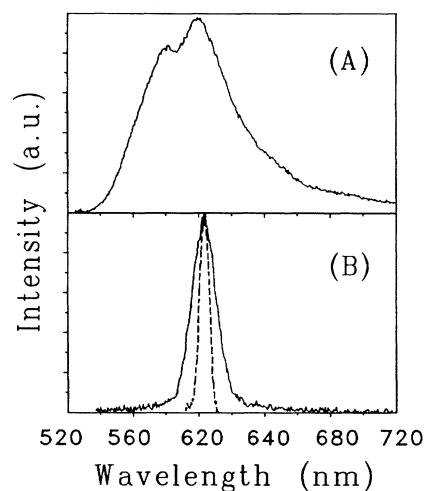


FIG. 3. Emission spectra of *R*-PE single crystal at room temperature: (a) exciton band appears at 600 nm at pump density of 1 GW/cm^2 ; and (b) exciton superradiance at 12 GW/cm^2 (solid line), and 30 GW/cm^2 (dashed line).

shown in Fig. 4(a). When the pump density is higher than 7 GW/cm^2 , the emission only appears at the exciton band, and the lifetime of the emission is as short as the pump pulse duration, as shown in Fig. 4(b).

(4) The higher the pump density, the sharper the emission spectrum. Typically, when the pump density is 12 GW/cm^2 , the emission bandwidth for the bulk crystal is 13 nm; when the pump density is 30 GW/cm^2 , the emission bandwidth sharpens to 7 nm, as shown in Fig. 3(b). However, the bandwidth of the time-integrated emission spectrum is larger than 4.4 nm in spite of the higher pump density because of frequency chirping.

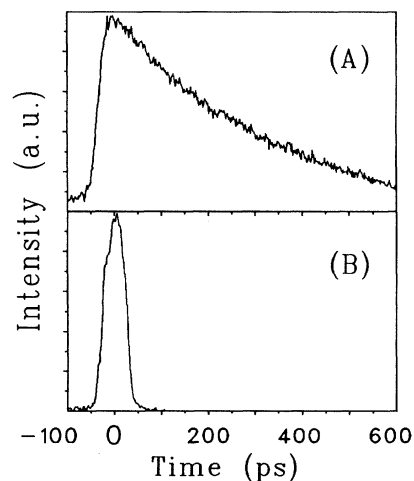


FIG. 4. Emission decay curves of *R*-PE single crystal at room temperature: (a) at low excitation density (0.1 W/cm^2 , pulse train); and (b) superradiance emission decay at high pump density (12 GW/cm^2 , single pulse).

(5) With respect to the peak of the emission pulse, a redshift at the rise time and a blueshift at the fall time of the emission pulse are observed (as shown in Fig. 5). This frequency chirping is one of the characteristics of Frenkel exciton superradiance.

We focus upon a coherent process of the excitons after the excitation pulse. It is appropriate to establish a two-level model for chromophores in *R*-PE, and make the approximation that the chromophores attached to the polypeptides in the *R*-PE crystal with regular geometry (*R3* space group) [25] are identical in energy state structure.

The Hamiltonian of *N* initially excited chromophores in an *R*-PE crystal mutually interacting with the external radiation field is given by

$$H = H_E + H_R + H_I, \quad (1.1)$$

where H_E , H_R , and H_I are the Hamiltonians of the excitons, the radiation field, and the interaction between field and excitons, respectively,

$$H_E = \hbar\omega_0 \sum_{j=1}^N D_j, \quad (1.2)$$

$$H_R = \sum_{\epsilon,k} \hbar\omega_k (a_{\epsilon k}^\dagger a_{\epsilon k} + \frac{1}{2}), \quad (1.3)$$

$$H_I = - \sum_{j=1}^N [E^+(r_j) + E^-(r_j)] D_{Ej}. \quad (1.4)$$

In the above equations, $\hbar\omega_0$ is the energy corresponding to the incoherent transition of a single excited chromophore, D_j the diagonal density operator of excitons, and $a_{\epsilon k}^\dagger$ and $a_{\epsilon k}$ denote the creation and annihilation operators acting on the mode of the field with wave vector k , polarization ϵ , and photon energy $\hbar\omega_k$. D_{Ej} stands for the chromophore transition dipole moment interacting with fields $E^+(r_j)$ and $E^-(r_j)$ at the j th chromophore site.

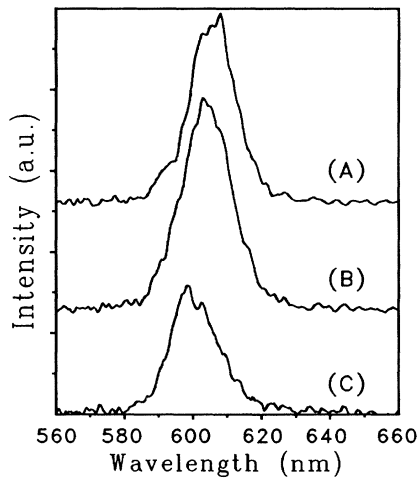


FIG. 5. Redshift and blueshift of Frenkel exciton superradiance in *R*-PE crystal at 12 GW/cm² pump density: spectra at the rise time (a), at the peak (b), and at the fall time (c) of the emission pulse, respectively.

The master equation of the exciton density operator (under the Born-Markov approximation) [12,26] is

$$\begin{aligned} \frac{d\rho}{dt} = & -\frac{\Gamma}{2} \sum_{ij} [D_i^+ D_j^-, \rho]_+ + \Gamma \sum_{ij} D_j^- \rho D_i^+ \\ & + \frac{1}{i\hbar} \sum_{i>j} [\Omega_{ij} D_i D_j, \rho]_-, \end{aligned} \quad (2)$$

where Γ and Ω_{ij} , respectively, stand for the spontaneous emission rate of a single excited chromophore and the dipole-dipole interaction between excited chromophores i and j with displacement r_{ij} ,

$$\Gamma = \frac{8\pi^2 d^2}{3\epsilon_0 \hbar \lambda^3}, \quad (3.1)$$

$$\Omega_{ij} = \frac{d^2}{4\pi\epsilon_0 |r_{ij}|^3} \left[\epsilon_i \cdot \epsilon_j - 3 \frac{(\epsilon_i \cdot r_{ij})(\epsilon_j \cdot r_{ij})}{|r_{ij}|^2} \right], \quad (3.2)$$

with d and λ denoting the magnitude of the transition dipole moment and the transition wavelength, and $\epsilon_{i,j}$ the unit vectors along the directions of the transition dipole moments of the i th and j th excited chromophores.

Generally, the dipole-dipole interaction operator Ω may break the permutation symmetry of the chromophore-field coupling, leading to a loss of dipole-dipole correlation. However, preliminary crystallographic studies [25] reveal that the pattern of chromophore location in the *R*-PE crystal can be approximated as a multiring pattern, in which the plane of each ring is perpendicular to the c axis, whereas the c component of each chromophore transition dipole is dominant over the ab component. For two nearest neighbor excited chromophores,

$$\Omega_{ij} = \frac{d^2}{4\pi\epsilon_0 r^3} \xi(\theta, \eta), \quad (4)$$

where $r = |r_{ij}|$ and $\xi(\theta, \eta) = (\frac{5}{2} \cos\theta - \frac{3}{2}) \cos\eta$ describes the orientation contribution of the dipole moments, while θ and η are the angles between the dipole moments and between the dipole moment and c axis. Therefore dipole-dipole interaction perturbation satisfies the permutation symmetry of the chromophore-field coupling, and complete decorrelation may not occur. In other words, superradiance may be observed. In addition, we have measured the fluorescence polarization of the *R*-PE single crystal with different orientation of the c axis with respect to the excitation polarization, and found that $\xi(\theta, \eta) > 0$.

Expanding the dipole-dipole interaction perturbation Ω in the Dicke basis [1,26] yields

$$\langle JM | \hbar\Omega | JM \rangle = \frac{\zeta \xi d^2}{4\pi\epsilon_0 r^3} \frac{J^2 - M^2}{J - \frac{1}{2}}, \quad (5)$$

where ζ is dependent on the effective number of chromophore rings. According to Eq. (5), the energy of the ℓ th photon emitted via superradiance is [26]

$$\hbar\omega_\ell = -\frac{\zeta \xi d^2}{4\pi\epsilon_0 r^3} \left(1 - \frac{2\ell}{N} \right). \quad (6)$$

Therefore,

$$\hbar \omega_\ell \begin{cases} < 0 & \left(1 \leq \ell < \frac{N}{2}\right), \\ = 0 & \left(\ell = \frac{N}{2}\right), \\ > 0 & \left(\frac{N}{2} < \ell \leq N\right). \end{cases} \quad (7.1)$$

$$\hbar \omega_\ell \begin{cases} < 0 & \left(1 \leq \ell < \frac{N}{2}\right), \\ = 0 & \left(\ell = \frac{N}{2}\right), \\ > 0 & \left(\frac{N}{2} < \ell \leq N\right). \end{cases} \quad (7.2)$$

$$\hbar \omega_\ell \begin{cases} < 0 & \left(1 \leq \ell < \frac{N}{2}\right), \\ = 0 & \left(\ell = \frac{N}{2}\right), \\ > 0 & \left(\frac{N}{2} < \ell \leq N\right). \end{cases} \quad (7.3)$$

The relationships (7.1) and (7.3), corresponding to redshift and blueshift, respectively, are known as frequency chirping, which characterizes the interaction and coherence between chromophore dipole moments.

As shown in Fig. 3(b), the superradiance of excitons occurs at 603.5 nm, the red side of the exciton band, and the higher the pump density the sharper the emission band. These two properties of high density Frenkel excitons are similar to those of condensate bosons. However, the redshift and blueshift of the exciton superradiance reveal the nonboson properties. In a word, the experimental results imply that the high density Frenkel excitons may be deformed bosons.

In addition, as shown in Fig. 1, the absorption band [in Fig. 1(c)] of *C*-phycocyanin, the energy acceptor of *R*-PE in phycobilisome, covers the exciton band of *R*-PE much better than the monomolecular fluorescence band of *R*-PE [Fig. 1(a)]. This implies that an exciton mechanism can explain the high efficiency of energy transfer in photosynthetic antennae.

In summary, superradiance of high density Frenkel excitons in an *R*-PE crystal is observed at room temperature for the first time. The emission lifetime is shorter than the pump pulse duration. The bandwidth is narrower than the excitonic bandwidth, and the higher the pump density the sharper the emission band. A redshift at the rise time and a blueshift at the fall time of the superradiant emission pulse are observed. The experimental results also imply that the high density Frenkel excitons may be deformed bosons, and that excitons play an important role in energy transfer in algal photosynthetic antennae.

- [1] R. H. Dicke, Phys. Rev. **93**, 99 (1954).
- [2] N. Shribanowitz, I. P. Herman, J. C. MacGillivray, and M. S. Feld, Phys. Rev. Lett. **30**, 309 (1973).
- [3] M. S. Feld and J. C. MacGillivray, in *Coherent Nonlinear Optics*, edited by M. S. Feld and V. S. Letokhov (Springer-Verlag, New York, 1980), pp. 7–57.
- [4] Q. H. F. Vreken and H. M. Gibbs, in *Dissipative Systems in Quantum Optics*, edited by R. Bonifacio (Springer-Verlag, New York, 1981), pp. 111–147.
- [5] P. V. Zinóviev *et al.*, Sov. Phys. JETP **58**, 1129 (1984).
- [6] S. N. Andrianov *et al.*, Sov. Phys. JETP **64**, 1180 (1986).
- [7] R. Florian, L. O. Schwan, and D. Schmid, Solid State Commun. **42**, 55 (1982).
- [8] A. Schiller, L. O. Schwan, and D. Schmid, J. Lumin. **38**, 243 (1984).
- [9] L. O. Schwan, J. Lumin. **48**, 289 (1991).
- [10] F. C. Spano, J. R. Kuklinski, and S. Mukamel, Phys. Rev. Lett. **65**, 211 (1990).
- [11] H. Fidder and D. A. Wiersma, Phys. Rev. Lett. **66**, 1501 (1991).
- [12] T. Tokihiro, Y. Manabe, and E. Hanamura, Phys. Rev. B **47**, 2019 (1993).
- [13] Y. Manabe, T. Tokihiro, and E. Hanamura, Phys. Rev. B **48**, 2273 (1993).
- [14] H. Suzuura, T. Tokihiro, and Y. Ohta, Phys. Rev. B **49**, 4344 (1994).
- [15] E. Hanamura, Phys. Rev. B **38**, 1228 (1988).
- [16] T. Itoh, T. Ikehara, and Y. Iwabuchi, J. Lumin. **45**, 29 (1990).
- [17] S. D. Boer and D. A. Wiersma, Chem. Phys. Lett. **165**, 45 (1990).
- [18] H. Fidder, J. Knoester, and D. A. Wiersma, Chem. Phys. Lett. **171**, 529 (1990).
- [19] M. Hasuo *et al.*, Phys. Rev. Lett. **70**, 1303 (1993).
- [20] B. Link and G. Baym, Phys. Rev. Lett. **69**, 2959 (1992).
- [21] D. W. Snoke, J. P. Wolfe, and A. Mysyrowicz, Phys. Rev. B **41**, 11 171 (1990).
- [22] F. C. Spano, Phys. Rev. Lett. **67**, 3424 (1991).
- [23] J. L. Birman, Solid State Commun. **84**, 259 (1992).
- [24] B.-X. Li, Phys. Lett. A **155**, 313 (1991).
- [25] L. Liang and N.-J. Zhu, Scientia Sinica B **35**, 58 (1992).
- [26] M. Gross and S. Haroche, Phys. Rep. **93**, 301 (1981).